HHS Public Access

Author manuscript

Macromol Biosci. Author manuscript; available in PMC 2023 July 01.

Published in final edited form as:

Macromol Biosci. 2022 July ; 22(7): e2200067. doi:10.1002/mabi.202200067.

Angiogenic Hydrogels to Accelerate Early Wound Healing

KaKyung Kim[^,1], **Zain Siddiqui**[^,1], **Amanda M. Acevedo-Jake**[1], **Abhishek Roy**[1], **Marwa Choudhury**[1], **Jonathan Grasman**[1], **Vivek Kumar**[1,2,3,4,*]

[1]Department of Biomedical Engineering, New Jersey Institute of Technology, Newark, NJ 07102, USA

[2]Department of Biology, New Jersey Institute of Technology, Newark, NJ 07102, USA

[3]Department of Chemical Engineering, New Jersey Institute of Technology, Newark, NJ 07102, USA

[4]Department of Restorative Dentistry, Rutgers School of Dental Medicine, Newark, NJ 07102, USA

Abstract

The metabolic disorder diabetes mellitus affects an increasing proportion of the population, a number projected to double by 2060. Non-life-threatening comorbidities contribute to an interrupted healing process which is first delayed, then prolonged, and associated with increased susceptibility to infection and sustained and unresolved inflammation. This leads to chronic non-healing wounds and eventually potential amputation of extremities. Here we examine the use of a bioactive angiogenic peptide-based hydrogel, SLan, to improve early wound healing in diabetic rats, and compare its performance to clinically utilized biosynthetic peptide-based materials such as Puramatrix. Streptozotocin-treated diabetic rats underwent 8 mm biopsy wounding in their dorsum to remove the epithelium, adipose tissues and muscle layer of the skin, and served as a model for diabetic wound healing. Wounds were treated with either Low (1w%) SLan, High (4w%) SLan, PBS, Puramatrix or K2 (an unfunctionalized non-bioactive control sequentially similar to SLan), covered with Tegaderm and monitored on days 0, 3, 7, 10, 14, 17, 21, 28; animals were sacrificed for histomorphic analyses and immunostaining. An LC/MS method developed to detect SLan in plasma allows pharmacokinetic analysis showing no trafficking of peptides from the wound site into the circulation. Low and High SLan groups show similar final outcomes of wound contraction as control groups (Puramatrix, PBS and K2). SLan-treated rats, however, show marked improvement in healing in earlier time points, including increased deposition of new mature blood vessels. Additionally, rats in the Low SLan treatment groups showed significantly improved wound contraction over other groups and significantly improved healing in early time points. Altogether our results suggest this material can be used to ‘jumpstart’ the diabetic wound healing process.

Graphical Abstract

[*]Correspondence: vak@njit.edu.
[^]These authors contributed equally for co-first author

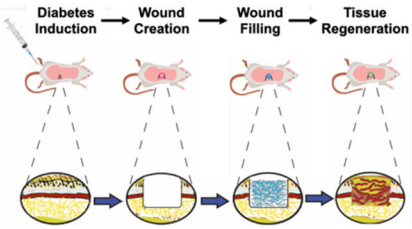

Angiogenesis in early wound healing model is critical to cellular infiltration, survival and neo-matrix deposition. Angiogenic hydrogels based on self-assembling peptides show rapid neovascularization and wound healing in a rodent diabetic wound healing model.

Keywords

Angiogenesis; Peptide; Hydrogel; Wound healing; VEGF

INTRODUCTION

Diabetes mellitus (DM) is one of the most prevalent metabolic disorders worldwide, is caused by hyperglycemia, and affects ~35 million Americans, a figure slated to double by 2060 [1, 2], and which has a global annual cost ~$250 billion [3, 4]. Diabetic patients suffer from many non-life-threatening complications resulting from DM including diabetic nephropathy, cardiovascular co-morbidities, neuropathy, and limb ischemia or even amputation [5]. Chronic wounds arise from diabetic foot ulcers (DFUs), developed by nearly 19–34% of diabetics in their lifetime, and of which 65% of patients likely to suffer a recurrence within 5 years [6]. Wound healing in diabetics is hindered by a combination of neuropathy, vasculopathy, infection, and other intrinsic and extrinsic factors due to hyperglycemia, advanced glycation end-products (AGEs) and other diabetes-related pathophysiologies [7]. The normal healing process in acute cutaneous wounds proceeds in four distinct phases: hemostasis, inflammation, proliferation including re-epithelialization and granulation, and finally remodeling [7–9]. In diabetic wound healing, however, this repair mechanism does not proceed linearly or synchronously, resulting in a prolonged, sustained inflammation and hypoxia, which leaves the wound vulnerable to further complications and infection [7, 10]. Additionally, hyperglycemia can induce peripheral neuropathy which narrows blood vessel and alters perfusion – exacerbating ulceration [10–12].

Microvascular changes include a reduction in capillary size and alteration of a vessel's basement membrane due to ischemia [7], and do not include other concomitant unwanted co-morbidities ensuing from cardiovascular/ peripheral vascular atherosclerotic disease which lead to vessel inflammation, platelet aggregation, and endothelial dysfunction [7, 9, 13–15]. Tissue vascularization is slowed by a deficiency of vascular endothelial growth factor (VEGF) in the injury site [4, 9, 16–18]. VEGF is a key mediator modulating angiogenesis during the proliferative stage of wound healing [19, 20]. When cutaneous injury occurs, the immediate change to hypoxic conditions induces a variety of cells (i.e. keratinocytes, fibroblasts, endothelial cells, macrophages, and platelets) to release VEGF

[9, 21]. VEGF facilitates vascularization by promoting angiogenesis and vasculogenesis, and increases blood vessel permeability to improve cellular infiltration at the injury site, crucial for local repair [9, 17, 18, 21]. Previous studies have shown that topical VEGF applications can accelerate chronic wound healing in diabetic mice [16, 17]. While promising, the clinical application of such factors alone without a more effective delivery method leaves this treatment modality limited [18, 22, 23]. Currently these therapies have significant disadvantages, however, including off-target signaling and low persistent local concentrations at the tissue regeneration site, and are also cost prohibitive [24–27].

Current standard of care for diabetic wound treatment involves a combination of vascular examination for assessment, followed by infection management, debridement, offloading, and dressing application [28]. Despite the effectiveness of these methods, nearly 20% of DFUs still result in a lower extremity amputation [6]. As mentioned previously, topical application of growth factors like VEGF show promise, though studies report conflicting evidence about their overall efficacy [10, 29, 30], potentially limited by the transient localization of growth factor in the area [29, 31, 32]. These limitations thus tend to require repeat dosing which increase treatment costs [29]. Other pro-angiogenic approaches employing gene therapy and stem cell administration [33–36] have demonstrated limited clinical effectiveness due immune rejection, poor gene uptake and maladaptive inflammatory responses [37–42]. Therefore, there is a clear need for an alternative approach which can guide the formation of new vasculature and accelerate tissue repair through local presentation of a VEGF signal.

Biomaterials, such as self-assembling peptide hydrogels (SAPHs), have shown promise as alternatives to growth factor delivery for wound healing [43–45]. SAPHs are composed of multiple short repetitive peptide domains directing monomer self-assembly to large ordered nanofibers via non-covalent interactions [46], and which further crosslink in three dimensions to form stable nanofibrous hydrogels [47–49]. These materials' porosity, tunability, biocompatibility, and injectability make them promising approaches for drug delivery, tissue regeneration, and other therapeutic needs [47, 49]. Specifically, regarding wound healing, SAPHs have been shown to offer better targeted delivery and longer-lasting therapeutic effects [29, 31, 32, 43, 45]. Our group has previously developed a pro-angiogenic SAPH (SLan) which encourages rapid and robust localized vascularization in several disease applications, including the ischemic tooth (canine), retina (rat), subcutaneous space (rat and mouse), cranial space (rat) to name a few [50–54]. This SAPH contains a self-assembling domain, K-$(SL)_6$-K, which directs the self-assembly of ß-sheet-forming peptide monomers into short nanofibers in aqueous solutions and a terminal angiogenic domain, "QK": KLTWQELYQLKYKGI, derived from VEGF-165 [46, 55]. Herein, we investigate the therapeutic efficacy of our pro-angiogenic peptide SLan against commercially available Puramatrix™ and a peptide control of the base self-assembly domain alone (named K2) for the acceleration of cutaneous wound healing in a diabetic wound healing rodent model (Figure 1).

METHOD & MATERIALS

Synthesis

Peptides were synthesized at 0.1 mM scale on a CEM LibertyBlue solid phase peptide synthesizer using standard Fmoc chemistry. All peptides were C-terminally amidated and N-terminally acetylated. The crude peptides were cleaved with a mixture of 2.5% H_2O, 2.5% triisopropylsilane, 2.5% 3,6-dioxa-1,8-octanedithiol and 92.5% trifluoroacetic acid (10 mL total) for 30 min at 37°C. The cleaved crude peptides were triturated with cold ether then centrifuged to form a pellet; the ether was then decanted, and the peptide left to dry overnight. The resulting crude pellet was dissolved in Milli-Q water at a concentration of ~1 mg/mL, adjusted to neutral pH, and dialyzed (Spectra Por S/P 7 RC dialysis tubing, 2000 MWCO) against DI water for 3 days (total reservoir volume 30L, changed 3 times a day). Next, the peptide was frozen at −80°C overnight and then lyophilized to give a white powder. Peptide identity was confirmed by an Orbitrap Q Exactive LC/MS (Thermo Scientific, Waltham, MA). To verify commercial manufacturing potential, peptides also were manufactured at gram-scale with similar purity (>90%) by AmbioPharm Inc (Beech Island, SC).

Rodent diabetic dermal wound healing model

All studies were approved by the Care Research, LLC IACUC (Fort Collins, CO) which performed the dermal wound healing model in rats. To induce diabetes, a single 65 mg/kg IV dose of Streptozotocin (STZ) was injected into Sprague Dawley rats. A 50 mM sodium citrate buffer was used to formulate STZ to a concentration of 50 mg/mL. The volume of 1.0 mL/kg of STZ was diluted to produce a dosage of 65 mg/kg per rat. Blood glucose level was measured prior to STZ injection, and again on day 3, 7 and 11 post STZ injection via tail vein puncture. The rats with blood glucose level of 300–600 mg/dl were randomized and enrolled into each group: PBS, K2, PuraMatrix™ hydrogel, 1 w% Slan (SLan-Low) or 4 w% Slan (SLan-High) (Table 1). A single full thickness 8 mm biopsy punch was created on the shaved dorsal back of each anesthetized rat. Each rat was enrolled in a specific topical treatment of the wound site, 200μL of each medicament was applied intradermally and the wound was covered with Tegaderm™ (3M) dressing. Wounds were checked daily and filled with respective medicament groups at Day 3 or 5. No additional filling of wound was performed past day 7. (only PBS had to be reapplied at day 3 and 5 due to the inviscid nature of the buffer. Analgesic and antibiotics were administered for 2–3 days post wound creation. on days 1, 3, 7, 14 and 28 post-wound puncture, wound pictures and blood samples were taken. Rats were euthanized and the wound sites were explanted and placed in 10% formalin for histological analysis on day 28 post-wound puncture.”

Pharmacokinetics sampling and analysis

Rat blood samples from 1 and 4 w.% SLan treated groups were taken from the tail vein on 1, 3, 7, 14 and 28 days It was collected in K2EDTA anticoagulant tubes, plasma was obtained and frozen in −80°C. A liquid chromatography electron spray ionization (LC/ESI-MS) method was developed (presented in SI Figure 1) for quantifying the peptides in the plasma concentration ranging from 1000 to 10 ng/ml (data shown in SI Figure 2). Concentrations below 10 ng/ml were found to be below the detection limit for plasma.

Histology

Explants of skin samples at the terminal end pointwere collected, fixed in formalin, embedded in paraffin blocks, sectioned to 6–8μm and then stained with hematoxylin and eosin (H&E), Masson's Trichrome (MT) (SigmaAldrich, St. Louis, MO). For immunostaining, primary antibodies were diluted in antibody buffer and the sections were incubated overnight at 4°C. The sections were washed in phosphate buffered saline (PBS) 3 times followed by secondary antibodies and incubated at room temperature for 45 minutes. DAPI Antifade® mounting medium containing DAPI was added dropwise before coverslipping. Panel of antibodies used include: Mouse anti-rat CD31 (Southern Biotech, Birmingham, AL) and rabbit anti-rat α-SMA (ThermoFisher, Waltham, MA) at 1:20 and 1:100 dilution, respectively, as per the manufacturers' recommendation. The secondary antibodies used were fluorescein isothiocyanate (FITC) donkey-anti rabbit for α-smooth muscle active (α-SMA) and Texas Red goat anti-mouse at 1:1000 dilution factor for both.

Quantification of Wound Healing and Blood Vessel Density

On days 3, 7, 10, 14, 17, 21, 24 and 28, wound sizes were measured cranio-caudally and with digital calipers. Photographic analysis was used to measure the wound area on days 0, 3, 7, 10, 14, 17, 21, 24 and 28 (Figure 2). To evaluate wound contraction, the calculated areas were normalized to the area of day 0 and calculated into percentages (SI Figure 3). To quantify wound healing, MT-stained tissue sections from the terminal endpoints were scanned using Leica Aperio Imagescope. ImageJ was used to evaluate wound closure, dermal thickness, and distance between regenerated dermal muscle (mm). The gap between left and right epithelial tongues was measured to evaluate wound closure. The vertical distance from epithelium to border of regenerated dermal and muscle tissue was measured to determine the dermal thickness. The gap between the regenerated muscles was estimated to establish the lack of regenerated dermal muscle. The total area of regenerated tissue was measured using Photoshop. The number of pixels was converted to mm^2 by dividing each pixelated area by scale bar pixel area and multiplying the scale bar area in mm^2.

Statistical Analysis

Experiment data are presented as mean ± Standard Error Mean (SEM). Shapiro-Wilk for each group and Levene's test were used to determine normality and homogeneity of variance. One-way ANOVA was used for multiple comparisons of parametric data, with a Tukey post-hoc analysis when samples are normal and homogeneous. For the data that violate normality, non-parametric tests, Kruskal-Wallis Test with Post-hoc was used. The data violating homogeneity were determined using Welch's F-test with Post-hoc.

RESULTS

Previous studies have shown that SAPHs support cell growth, proliferation and cellular infiltration in a subcutaneous implant *in vivo* models [56]. Carrejo et al. evaluated K2 as a diabetic wound dressing and observed the greatest depth of granulation tissue complimented by degradation of SAPH and a high cellular density throughout the wound bed [57]. Additionally, SLan showed promoted angiogenesis demonstrated both *in vitro* and *vivo* models [58], and confirm the correct mass and purity with LC/MS techniques (Figure S1) as

well as the localization of the hydrogel SLan to the wound bed (SI Figure 2). As one of our previous studies showed efficacy of SLan in dental pulp regeneration in canines [54], here we have focused on application of this proangiogenic hydrogel in diabetic wound healing.

Analysis of Wound Contraction

To examine the effects of wound contraction and closure between different treatments, PBS, SLan Low, SLan High, Puramatrix and K2 (Table 1), images of wounds were taken on day 0, 3, 7, 14, and 28 (Figure 2A). While each treatment condition resolved wound closure by day 28, visual inspection of the wounds suggested that the kinetics of wound closure were impacted by treatment with SLan (Figure 2A). Monitoring to final time points reveals full wound contraction and closure in all groups and show no significant differences between groups at day 28 (Figure 2B). Importantly, treatment with a low concentration of SLan was shown to significantly expedite wound closure at early days 3, 7, and 14 after injury with respect to PBS (SI Figure 3). Hydrogel treatment groups show improved wound closure overall compared to PBS. In particular, SLan Low significantly accelerated wound healing over PBS, clearly evident by day 3. By day 14, low and high SLan treated groups promoted an elevated wound closure (76.2% and 74.5% wound contraction respectively) while PBS, Puramatrix and K2 resulted in 64.5%, 68.6%, and 69.6% contraction. Overall, in early phase through day 3 to day 14, SLan Low (1 w% only) show significant differences compared to PBS. Although both 1 w% and 4 w% SLan groups show rapid wound closure at early time points (day 3 to 14) compared other control conditions, they reached comparable wound closure to SLan at later time points (day 21 and 24) and all groups showed full wound closure by day 28.

Quantification of Wound Healing and Evaluation of Angiogenesis

Rats were sacrificed for wound site histological evaluation and did not show a significant change in the body weight (SI Figure 4), signs of inflammation or changes in behavior of any of the groups over the course of the study. The histology was used to evaluate epithelium regeneration, granulation tissue reformation and angiogenesis (Figure 3). MT-stained sections were analyzed to quantify dermal thickness, regenerated tissue area in wound bed and gap distance between regenerated muscle in dermal area (Figure 3A). At the terminal timepoint, wounds in all groups fully regenerated granulation tissue as the newly deposited granulation tissues in wound bed reached equivalent levels as in the adjacent native tissue. H&E and MT staining show complete regeneration of epithelium on wound site forming barriers between wound areas and outside environment of all groups. Furthermore, MT visualizes collagen formation within the wound bed.

To maintain live and healthy regenerated granulation tissue, blood vessels within the wound bed must be formed. Day 31 MT images were further analyzed to evaluate blood vessel formation within the wound bed (Figure 3H). Average of blood vessel formation in wound bed were quantified to be 35.1% and 26.1% for SLan Low and High, respectively when number of blood vessel in the wound bed divided by the area at the terminal time point, while PBS, Puramatrix and K2 were evaluated to be 11.4%, and 7.2% respectively. Both low and high weight percentage SLan significantly promoted local angiogenesis compared to control groups (PBS, Puramatrix, and K2). Notably, neo blood vessels were homogeneously

formed throughout the wound bed for SLan groups while in other control groups vessels were formed near edges of wounds.

To qualitatively evaluate degree of angiogenesis in High SLan (4 w%) group, immunostaining for endothelial cells that line blood vessels and blood vessel maturity indicated by a surrounding layer smooth muscle cells were stained for using CD31 and α-SMA, respectively (Figure 4). Also, slides were counterstained with DAPI to identify nuclei. For Angiogenic SAPH scaffolds, we observed a large density of vessels in the regenerated tissue with hair follicles in native tissue as shown in Figure 4A along with regeneration of numerous neo-vessels in the wound gap as shown in Figure 4B. Similar immunostaining was performed for Low SLan (1 w%) group (Figure S6).

Discussion:

Hydrogels, unlike traditional wound dressing such as bandages and gauzes, can be formulated to be biocompatible, biodegradable, injectable and antibacterial [4, 59]. Hydrogels have been actively studied for application of a wound healing dressing as they form localized physical barriers between wound and external environment which promote gas exchange, absorb excessive exudate and maintain moist environment, all mandatory features of native wound healing [60, 61].

Hydrogels have been made of various materials such as peptides, DNA, chitosan, alginate and many other biomaterials, as well as promoting self-assembly through pH and temperature adjustment [4]. The Ma group showed that their self-healing hydrogel composed of benzaldehyde group functionalized poly(ethylene glycol)-co-poly(glycerol sebacate) (PEGS-FA) induced outstanding blood clotting and significantly improved wound healing, collagen deposition and granulation formation by upregulating growth factors including VEGF [62].

Self-assembling peptide hydrogels (SAPHs) are used in various fields including three dimensional tissue cell culture, tissue repair and tissue engineering [63]. These SAPHs primarily have β-sheet structure as a molecular basis and designed to construct three dimensional scaffolds [64]. RADA16 is an example of commercially available SAPHs that are currently used in clinics. RADA16 functions as a topical hemostatic agent for surgery and prevents adhesion formation after surgery [65]. Previously the Hartgerink group studied diabetic wound healing in mice with SAPH composed of self-assembling domain without the biological mimics with significantly accelerated wound closure in their SAPH, K2, compared to a commercially available hydrogel, IntraSite and buffer groups [57]. SAPHs, including RADA16 and K2, can be modified with various functional peptides to develop bioactive SAPHs imbued with the abilities of the appended mimetic sequence. In our work here, SAPHs (composed of a self-assembling domain and terminal bioactive VEGF epitope domain, SLan) were applied on wound of diabetic rodents and compared to K2, Puramatrix and PBS. SLan, the angiogenic peptide, showed significant acceleration in wound closure within the first two weeks of healing, compared to other groups. Additionally, a higher percent angiogenic hydrogel (SLan High) promoted rapid healing at early time points

similar to SLan Low. At later time points, there are no differences between groups and all groups tested exhibited full wound closure by the terminal timepoint.

Formation of new blood vessels in the wound was observed during skin wound healing. VEGF is implicated in the beginning of angiogenesis within the wound and is known to be a main factor regulating wound healing. VEGF is involved in numerous signaling cascades in wound healing angiogenesis including vasodilation, membrane degradation, endothelial cell proliferation and membrane formation [66–72]. Moreover, recently, VEGF has been shown to contribute to epithelization and collagen deposition [73]. Impaired wound healing mechanisms in DFU patients cause diminished angiogenesis and reduced peripheral blood flow resulting in lack of healing at the wound site [74]. Studies have shown that level of VEGF is significantly diminished in wounds of *db/db* mice compared to healthy mice and VEGF treatment on *db/db* mice accelerated wound healing [75, 76]. In our study treating skin wounds in a STZ rat model with low and high SLan concentrations, we observed significantly higher angiogenesis and tissue regeneration within the wound bed and distributed through the wound compared to other groups. In addition, by day 31, the wound bed regenerated granulation tissues similar to the adjacent native tissue, while complete epithelium regeneration and collagen formation in wound bed were shown in all groups. Immunostaining of the SLan group displayed a large number of cellular infiltrations, as indicated by DAPI, within the regenerated wound bed complemented by degradation of the hydrogel. To further evaluate the fibrotic scar of a wound, lymph angiogenesis, immune cell infiltration, and other notable niche and cells types must be probed to fully understand scaffold efficacy potentially by immunostaining with respective markers or fluorescent activated cell sorting [77].

Conclusion:

There is considerable promise in the field of soft biomaterials for wound bed regeneration through the controlled delivery of essential growth factors, such as VEGF. However, tunable matrices, perhaps with multiple growth factors being delivered, modulating stiffness and the use of two-component hybrid scaffolds (combination of traditional scaffolds with soft biomaterials) may aid in increased angiogenesis at the wound site. Further, eliciting multiple signals for re-epithelization, follicular generation, and designing biocompatible materials that eliminate fibrotic tissue may also provide an ideal tissue regeneration platform/therapy. While angiogenic modulation of wound beds is critical to enhancing wound healing, a growing number of studies have also shown the importance of immune modulation. Future studies utilizing scaffolds to bind chemoattractants to modulate immune cell infiltration [78] or to modulate their activity and resultant phenotype [50] can be envisioned and may provide synergistic enhancement of angiogenic and inflammation mediated wound healing. Overall in our study we have shown that treatment with SLan significantly improves wound healing in a diabetic rat model, as well as the deposition of neovessels in the wound bed. In particular, treatment with SLan speeds up early wound closure and healing and these treatment groups show robust re-epithelialization of the wound bed. While it is currently unclear why the Low SLan treatment groups outperform the High SLan groups, both groups show improved healing over controls and increase the blood vessel density in the dermal gap. On-going studies will elucidate these differences, as well as controlling the tunability

of the healing response, both through improved angiogenic sequence presentation and its combination with one or more other signaling scaffolds (for example scaffolds to modulate immune cell infiltration).

Supplementary Material

Refer to Web version on PubMed Central for supplementary material.

Glossary

DM	Diabetes mellitus
DFUs	diabetic foot ulcers
AGEs	advanced glycation end-products
VEGF	vascular endothelial growth factor
SAPHs	self-assembling peptide hydrogels
ACN	acetonitrile
STZ	streptozotocin
H&E	hematoxylin and eosin
MT	Masson's Trichrome
PBS	phosphate buffered saline
FITC	fluorescein isothiocyanate
SEM	standard error mean
PEGS-FA	poly(ethylene glycol)-co-poly(glycerol sebacate)

References

1. American Diabetes, A., Diagnosis and classification of diabetes mellitus. Diabetes Care, 2014. 37 Suppl 1: p. S81–90. [PubMed: 24357215]
2. Lin J, et al. , Projection of the future diabetes burden in the United States through 2060. Popul Health Metr, 2018. 16(1): p. 9. [PubMed: 29903012]
3. American Diabetes, A., Economic Costs of Diabetes in the U.S. in 2017. Diabetes Care, 2018. 41(5): p. 917–928. [PubMed: 29567642]
4. Kim K, et al. , Materials and Cytokines in the Healing of Diabetic Foot Ulcers. Advanced Therapeutics, 2021. 4(9): p. 2100075.
5. Guariguata L, et al. , Global estimates of diabetes prevalence for 2013 and projections for 2035. Diabetes Res Clin Pract, 2014. 103(2): p. 137–49. [PubMed: 24630390]
6. Armstrong DG, Boulton AJM, and Bus SA, Diabetic Foot Ulcers and Their Recurrence. N Engl J Med, 2017. 376(24): p. 2367–2375. [PubMed: 28614678]
7. Falanga V, Wound healing and its impairment in the diabetic foot. Lancet, 2005. 366(9498): p. 1736–43. [PubMed: 16291068]
8. Perez-Favila A, et al. , Current Therapeutic Strategies in Diabetic Foot Ulcers. Medicina (Kaunas), 2019. 55(11).

9. Brem H and Tomic-Canic M, Cellular and molecular basis of wound healing in diabetes. J Clin Invest, 2007. 117(5): p. 1219–22. [PubMed: 17476353]
10. Wang A, et al. , Guidelines on multidisciplinary approaches for the prevention and management of diabetic foot disease (2020 edition). Burns Trauma, 2020. 8: p. tkaa017. [PubMed: 32685563]
11. Chammas NK, Hill RL, and Edmonds ME, Increased Mortality in Diabetic Foot Ulcer Patients: The Significance of Ulcer Type. J Diabetes Res, 2016. 2016: p. 2879809. [PubMed: 27213157]
12. Al-Rubeaan K, et al. , Diabetic foot complications and their risk factors from a large retrospective cohort study. PLoS One, 2015. 10(5): p. e0124446. [PubMed: 25946144]
13. Marso SP and Hiatt WR, Peripheral arterial disease in patients with diabetes. J Am Coll Cardiol, 2006. 47(5): p. 921–9. [PubMed: 16516072]
14. Katakami N, Mechanism of Development of Atherosclerosis and Cardiovascular Disease in Diabetes Mellitus. J Atheroscler Thromb, 2018. 25(1): p. 27–39. [PubMed: 28966336]
15. Simons M, Angiogenesis, arteriogenesis, and diabetes: paradigm reassessed? J Am Coll Cardiol, 2005. 46(5): p. 835–7. [PubMed: 16139133]
16. Frank S, et al. , Regulation of vascular endothelial growth factor expression in cultured keratinocytes. Implications for normal and impaired wound healing. J Biol Chem, 1995. 270(21): p. 12607–13. [PubMed: 7759509]
17. Galiano RD, et al. , Topical vascular endothelial growth factor accelerates diabetic wound healing through increased angiogenesis and by mobilizing and recruiting bone marrow-derived cells. Am J Pathol, 2004. 164(6): p. 1935–47. [PubMed: 15161630]
18. Gurtner GC, et al. , Wound repair and regeneration. Nature, 2008. 453(7193): p. 314–21. [PubMed: 18480812]
19. Demidova-Rice TN, Hamblin MR, and Herman IM, Acute and impaired wound healing: pathophysiology and current methods for drug delivery, part 2: role of growth factors in normal and pathological wound healing: therapeutic potential and methods of delivery. Adv Skin Wound Care, 2012. 25(8): p. 349–70. [PubMed: 22820962]
20. Nissen NN, et al. , Vascular endothelial growth factor mediates angiogenic activity during the proliferative phase of wound healing. Am J Pathol, 1998. 152(6): p. 1445–52. [PubMed: 9626049]
21. Duffy AM B-HD, Harmey JH, Vascular Endothelial Growth Factor (VEGF) and Its Role in Non-Endothelial Cells: Autocrine Signalling by VEGF Landes Bioscience, 2000–2013.
22. Barrientos S, et al. , Clinical application of growth factors and cytokines in wound healing. Wound Repair Regen, 2014. 22(5): p. 569–78. [PubMed: 24942811]
23. Wietecha MS and DiPietro LA, Therapeutic Approaches to the Regulation of Wound Angiogenesis. Adv Wound Care (New Rochelle), 2013. 2(3): p. 81–86. [PubMed: 24527330]
24. Briquez PS, Hubbell JA, and Martino MM, Extracellular matrix-inspired growth factor delivery systems for skin wound healing. Advances in wound care, 2015. 4(8): p. 479–489. [PubMed: 26244104]
25. Babensee JE, McIntire LV, and Mikos AG, Growth factor delivery for tissue engineering. Pharmaceutical research, 2000. 17(5): p. 497–504. [PubMed: 10888299]
26. Martino MM, et al. , Growth factors engineered for super-affinity to the extracellular matrix enhance tissue healing. Science, 2014. 343(6173): p. 885–888. [PubMed: 24558160]
27. Lee K, Silva EA, and Mooney DJ, Growth factor delivery-based tissue engineering: general approaches and a review of recent developments. Journal of the Royal Society Interface, 2011. 8(55): p. 153–170. [PubMed: 20719768]
28. Frykberg RG and Banks J, Challenges in the Treatment of Chronic Wounds. Adv Wound Care (New Rochelle), 2015. 4(9): p. 560–582. [PubMed: 26339534]
29. Park JW, Hwang SR, and Yoon IS, Advanced Growth Factor Delivery Systems in Wound Management and Skin Regeneration. Molecules, 2017. 22(8).
30. Sridharan K and Sivaramakrishnan G, Growth factors for diabetic foot ulcers: mixed treatment comparison analysis of randomized clinical trials. Br J Clin Pharmacol, 2018. 84(3): p. 434–444. [PubMed: 29148070]

31. Losi P, et al. , Tissue response to poly(ether)urethane-polydimethylsiloxane-fibrin composite scaffolds for controlled delivery of pro-angiogenic growth factors. Biomaterials, 2010. 31(20): p. 5336–44. [PubMed: 20381861]
32. Chen RR and Mooney DJ, Polymeric growth factor delivery strategies for tissue engineering. Pharm Res, 2003. 20(8): p. 1103–12. [PubMed: 12948005]
33. Mohsin S, Wu JC, and Sussman MA, Predicting the future with stem cells. Circulation, 2014. 129(2): p. 136–8. [PubMed: 24249719]
34. Yasumura EG, et al. , Treatment of mouse limb ischemia with an integrative hypoxia-responsive vector expressing the vascular endothelial growth factor gene. PLoS One, 2012. 7(3): p. e33944. [PubMed: 22470498]
35. Sun Q, et al. , Sustained vascular endothelial growth factor delivery enhances angiogenesis and perfusion in ischemic hind limb. Pharm Res, 2005. 22(7): p. 1110–6. [PubMed: 16028011]
36. Sun Q, et al. , Sustained release of multiple growth factors from injectable polymeric system as a novel therapeutic approach towards angiogenesis. Pharm Res, 2010. 27(2): p. 264–71. [PubMed: 19953308]
37. Giacca M and Zacchigna S, VEGF gene therapy: therapeutic angiogenesis in the clinic and beyond. Gene Ther, 2012. 19(6): p. 622–9. [PubMed: 22378343]
38. Lu J, Pompili VJ, and Das H, Neovascularization and hematopoietic stem cells. Cell Biochem Biophys, 2013. 67(2): p. 235–45. [PubMed: 22038301]
39. Katare R, et al. , Clinical-grade human neural stem cells promote reparative neovascularization in mouse models of hindlimb ischemia. Arterioscler Thromb Vasc Biol, 2014. 34(2): p. 408–18. [PubMed: 24202301]
40. Stewart DJ, et al. , VEGF gene therapy fails to improve perfusion of ischemic myocardium in patients with advanced coronary disease: results of the NORTHERN trial. Mol Ther, 2009. 17(6): p. 1109–15. [PubMed: 19352324]
41. Simon-Yarza T, et al. , Vascular endothelial growth factor-delivery systems for cardiac repair: an overview. Theranostics, 2012. 2(6): p. 541–52. [PubMed: 22737191]
42. Kumar VA, et al. , Treatment of hind limb ischemia using angiogenic peptide nanofibers. Biomaterials, 2016. 98: p. 113–9. [PubMed: 27182813]
43. Lutolf MP and Hubbell JA, Synthetic biomaterials as instructive extracellular microenvironments for morphogenesis in tissue engineering. Nat Biotechnol, 2005. 23(1): p. 47–55. [PubMed: 15637621]
44. Balmayor ER, Targeted delivery as key for the success of small osteoinductive molecules. Adv Drug Deliv Rev, 2015. 94: p. 13–27. [PubMed: 25959428]
45. Carrejo NC, et al. , Multidomain Peptide Hydrogel Accelerates Healing of Full-Thickness Wounds in Diabetic Mice. ACS Biomater Sci Eng, 2018. 4(4): p. 1386–1396. [PubMed: 29687080]
46. Sarkar B, et al. , Membrane-Disrupting Nanofibrous Peptide Hydrogels. ACS Biomater Sci Eng, 2019. 5(9): p. 4657–4670. [PubMed: 33448838]
47. Lee S, et al. , Self-Assembling Peptides and Their Application in the Treatment of Diseases. Int J Mol Sci, 2019. 20(23).
48. Zhu J and Marchant RE, Design properties of hydrogel tissue-engineering scaffolds. Expert Rev Med Devices, 2011. 8(5): p. 607–26. [PubMed: 22026626]
49. Li J, et al. , Recent advances of self-assembling peptide-based hydrogels for biomedical applications. Soft Matter, 2019. 15(8): p. 1704–1715. [PubMed: 30724947]
50. Kumar VA, et al. , Self-assembling multidomain peptides tailor biological responses through biphasic release. Biomaterials, 2015. 52: p. 71–8. [PubMed: 25818414]
51. Kumar VA, et al. , Highly angiogenic peptide nanofibers. ACS Nano, 2015. 9(1): p. 860–8. [PubMed: 25584521]
52. Ma X, et al. , Angiogenic peptide hydrogels for treatment of traumatic brain injury. Bioact Mater, 2020. 5(1): p. 124–132. [PubMed: 32128463]
53. Sarkar B, et al. , Angiogenic Self-Assembling Peptide Scaffolds for Functional Tissue Regeneration. Biomacromolecules, 2018. 19(9): p. 3597–3611. [PubMed: 30132656]

54. Siddiqui Z, et al. , Angiogenic hydrogels for dental pulp revascularization. Acta Biomater, 2021. 126: p. 109–118. [PubMed: 33689817]
55. Aulisa L, Dong H, and Hartgerink JD, Self-assembly of multidomain peptides: sequence variation allows control over cross-linking and viscoelasticity. Biomacromolecules, 2009. 10(9): p. 2694–8. [PubMed: 19705838]
56. Petrak K, et al. , Challenges in Translating from Bench to Bed-Side: Pro-Angiogenic Peptides for Ischemia Treatment. Molecules, 2019. 24(7).
57. Carrejo NC, et al. , Multidomain Peptide Hydrogel Accelerates Healing of Full-Thickness Wounds in Diabetic Mice. ACS Biomaterials Science & Engineering, 2018. 4(4): p. 1386–1396. [PubMed: 29687080]
58. Siddiqui Z, et al. , Self-assembling Peptide Hydrogels Facilitate Vascularization in Two-Component Scaffolds. Chem Eng J, 2021. 422.
59. Kumar VA, et al., Injectable self-assembling antibacterial peptide hydrogels. 2020, Google Patents.
60. Eisenbud D, et al. , Hydrogel wound dressings: where do we stand in 2003? Ostomy/wound management, 2003. 49(10): p. 52–57.
61. Morton LM and Phillips TJ, Wound healing update. Semin Cutan Med Surg, 2012. 31(1): p. 33–7. [PubMed: 22361287]
62. Zhao X, et al. , Antibacterial anti-oxidant electroactive injectable hydrogel as self-healing wound dressing with hemostasis and adhesiveness for cutaneous wound healing. Biomaterials, 2017. 122: p. 34–47. [PubMed: 28107663]
63. Gelain F, Luo Z, and Zhang S, Self-assembling peptide EAK16 and RADA16 nanofiber scaffold hydrogel. Chemical Reviews, 2020. 120(24): p. 13434–13460. [PubMed: 33216525]
64. Gelain F, et al. , Self-assembling peptide scaffolds in the clinic. NPJ Regenerative Medicine, 2021. 6(1): p. 1–8. [PubMed: 33397999]
65. Gil ES, Aleksi E, and Spirio L, PuraStat RADA16 Self-Assembling Peptide Reduces Postoperative Abdominal Adhesion Formation in a Rabbit Cecal Sidewall Injury Model. Frontiers in Bioengineering and Biotechnology: p. 1302.
66. Nissen NN, et al. , Vascular endothelial growth factor mediates angiogenic activity during the proliferative phase of wound healing. The American journal of pathology, 1998. 152(6): p. 1445. [PubMed: 9626049]
67. Ferrara N and Henzel WJ, Pituitary follicular cells secrete a novel heparin-binding growth factor specific for vascular endothelial cells. Biochemical and biophysical research communications, 1989. 161(2): p. 851–858. [PubMed: 2735925]
68. Plouet J, Schilling J, and Gospodarowicz D, Isolation and characterization of a newly identified endothelial cell mitogen produced by AtT-20 cells. The EMBO journal, 1989. 8(12): p. 3801–3806. [PubMed: 2684646]
69. Yoshida A, Anand-Apte B, and Zetter BR, Differential endothelial migration and proliferation to basic fibroblast growth factor and vascular endothelial growth factor. Growth factors, 1996. 13(1–2): p. 57–64. [PubMed: 8962720]
70. Noiri E, et al. , Podokinesis in endothelial cell migration: role of nitric oxide. American Journal of Physiology-Cell Physiology, 1998. 274(1): p. C236–C244.
71. Senger DR, et al. , Tumor cells secrete a vascular permeability factor that promotes accumulation of ascites fluid. Science, 1983. 219(4587): p. 983–985. [PubMed: 6823562]
72. Senger DR, et al. , Purification and NH2-terminal amino acid sequence of guinea pig tumor-secreted vascular permeability factor. Cancer research, 1990. 50(6): p. 1774–1778. [PubMed: 2155059]
73. Stojadinovic O, A novel non-angiogenic mechanism of VEGF: Stimulation of keratinocyte and fibroblast migration. Wound Repair Regen, 2007. 15: p. A30.
74. Falanga V, Wound healing and its impairment in the diabetic foot. The Lancet, 2005. 366(9498): p. 1736–1743.
75. Seitz O, et al. , Wound healing in mice with high-fat diet-or ob gene-induced diabetes-obesity syndromes: a comparative study. Experimental diabetes research, 2010. 2010.

76. Galiano RD, et al. , Topical vascular endothelial growth factor accelerates diabetic wound healing through increased angiogenesis and by mobilizing and recruiting bone marrow-derived cells. The American journal of pathology, 2004. 164(6): p. 1935–1947. [PubMed: 15161630]

77. Lopez-Silva TL, et al. , Chemical functionality of multidomain peptide hydrogels governs early host immune response. Biomaterials, 2020. 231: p. 119667. [PubMed: 31855625]

78. Kim KK, et al. , A self-assembled peptide hydrogel for cytokine sequestration. J Mater Chem B, 2020. 8(5): p. 945–950. [PubMed: 31919489]

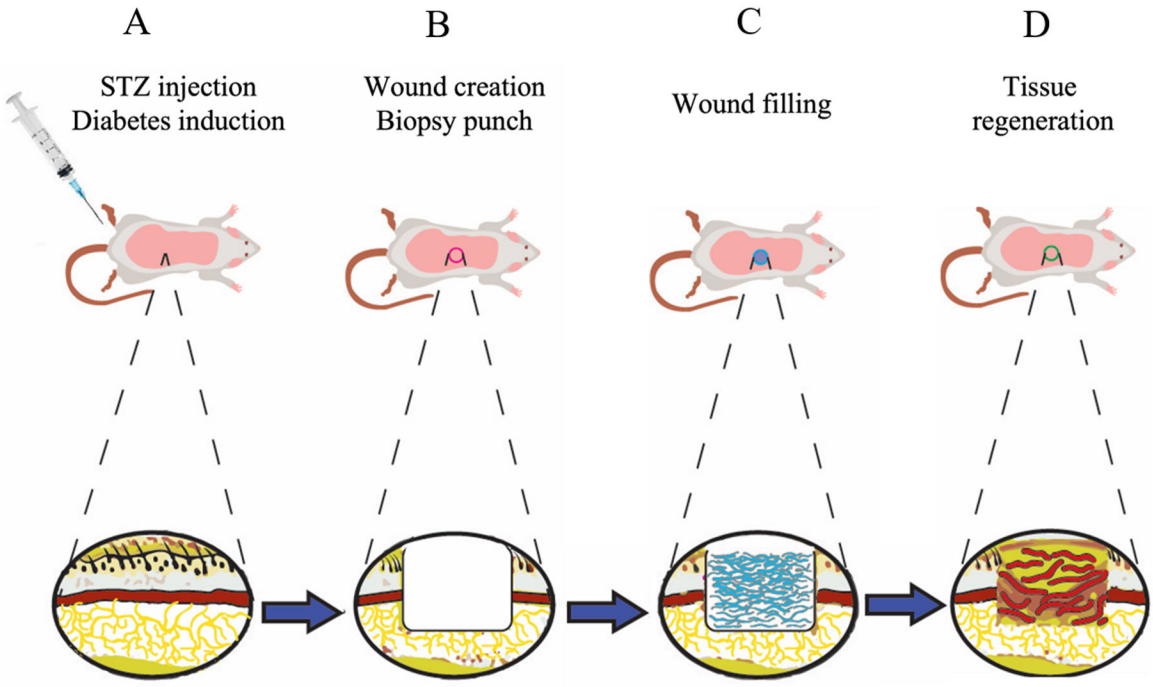

Figure 1. Schematic description of wound healing model.

(A) Diabetes was induced using streptozotocin (STZ) injection. (B) The randomized rats were subjected to an 8 mm biopsy wound in the dorsum, which removes epithelium, adipose tissue, and muscle layer as shown in cross-section. (C) The 5 different treatments including SLan Low, SLan High, K2, Puramatrix or PBS were applied, filled into these wounds, and covered with Tegaderm. (D) After 28 days, the wounds healed with newly deposited granulation tissue, collagen, and blood vessels.

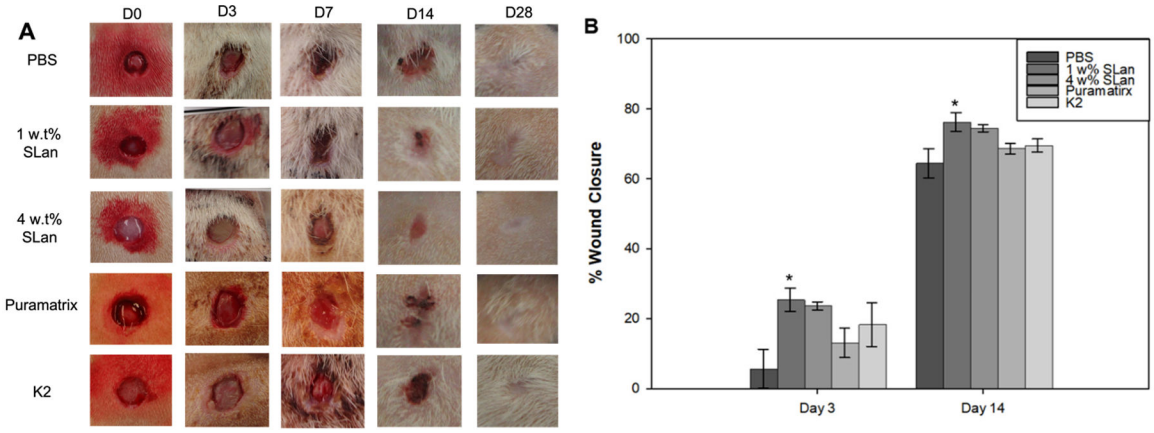

Figure 2. Quantification of wound closure.

(A) Photographs of wound closure showing full healing in all groups by 28 days. (B) Quantification of early phases of wound healing show a significant increase in wound closure in angiogenic hydrogels compared to carrier or other self-assembling peptide scaffolds. All wounds showed similar contraction by day 14 and had fully healed by Day 28 (Supplemental Figure 2).

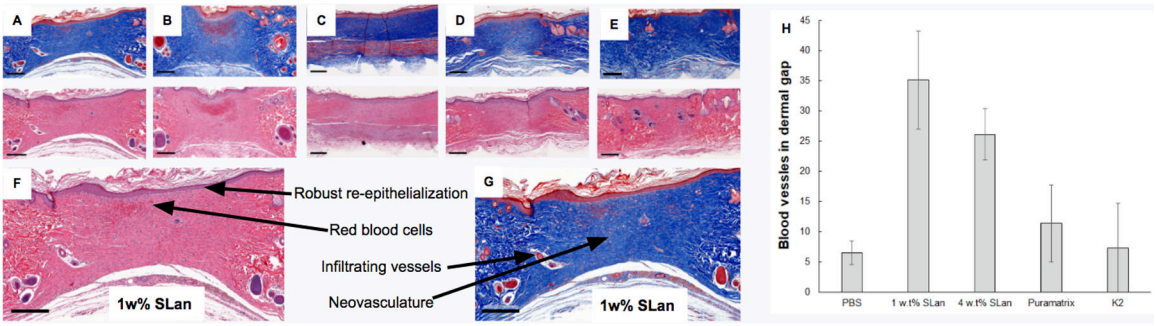

Figure 3. Histomorphometric characterization wounds.

Representative images of tissue sections of wounds treated with (A) 1 w% SLan, (B) 4 w% SLan, (C) K2, (D) Puramatrix and (E) PBS at day 31 contrasting the quality of regeneration at the tissue level. Both of H&E and MT stained tissue sections show complete wound closure at dermal gap (referring to regenerated dermal tissue site located at the center of histology images) at terminal explant (scale bars = 100 μm). (F,G) magnified sections of 1w% SLan H&E and MT stained sections show re-epithelialization, red blood cells, infiltrating vessels and neovasculature indicated by arrows (scale bars = 300 μm) (H) Blood vessels were observed and quantified in the granulation tissue using MT staining and counting of all groups - with significantly higher vessel density for SLan samples (n=8, *$p<0.05$).

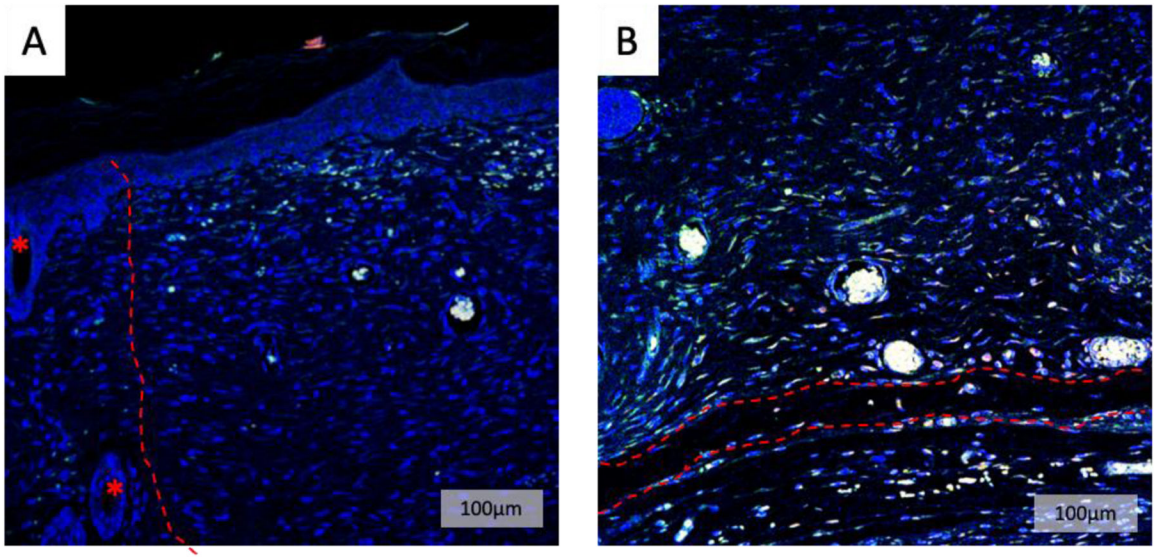

Figure 4. Immunofluorescent imaging of vascularization.

To further visualize vasculature, immunostaining for CD31 (red) and α-SMA (green) was performed on 4 w% SLan explants. (A) Low magnification images showed a large density of vessels in the regenerated tissue (right of dotted line) (* hair follicle in native tissue). (B) Neo-vessels within the wound bed were visualized at the base of the wound facing the subcutaneous space. The red dotted line represents vessels spanning the width of the wound gap.

Table 1.

Sample groups.

The following conditions were utilized in the rodent diabetic dermal wound healing model: PBS, SLan (1 and 4 w%), Puramatrix, K2.

Group	N	Type	Treatment
1	6	Negative Control	1x PBS
2	11	Test Article - Low Dose	SLan Low (10 mg/kg)
3	11	Test Article - High Dose	SLan High (40 mg/kg)
4	6	Comparator	PuraMatrix™
5	6	Comparator	K2 gel